Aerosol and Air Quality Research, 17: 84–97, 2017

ISSN: 1680-8584 print / 2071-1409 online
doi: 10.4209/aaqr.2016.01.0020

The Concentrations, Formations, Relationships and Modeling of Sulfate, Nitrate and Ammonium (SNA) Aerosols over China

Zhaoyu Cao[1], Xuehua Zhou[1*], Yujie Ma[1], Linpeng Wang[1], Ruidong Wu[1], Bing Chen[1*], Wenxing Wang[1,2]

[1] *Environment Research Institute, Shandong University, Shandong 250100, China*
[2] *Chinese Research Academy of Environmental Sciences, Beijing 100012, China*

ABSTRACT

Sulfate, nitrate and ammonium (SNA) are the dominant composition of secondary aerosols in the atmosphere and have a significant impact on public health, atmospheric chemistry process and climate. In this study, to evaluate SNA pollution in China, a first nationwide investigation derived from almost all published data in the field measurement before 2012 was carried out. The results show that SNA levels in China are about 3–5 times higher than those in USA and Europe. SNA account for 34.2 ± 10.9% in $PM_{2.5}$ and 28.2 ± 8.5% in PM_{10}. The highest SNA concentrations occur in urban areas of northern China. SNA all have peaks in winter, but the nadirs are in spring for sulfate and ammonium and in summer for nitrate. SOR (sulfur oxidation ratio) and NOR (nitrogen oxidation ratio) values show that the formations of sulfate and nitrate are distinct in different regions and seasons. The low average NO_3^-/SO_4^{2-} ratio (0.43 ± 0.26) indicates that the stationary emissions from coal combustion remain the main sources. There is a good relationship between ($2[SO_4^{2-}] + [NO_3^-]$) and $[NH_4^+]$ with near 1 slope, signifying that $(NH_4)_2SO_4$ and NH_4NO_3 are the predominant forms which SNA exist in particles in China. Based on the comprehensive observational data in China, the simulation for SNA aerosols by GISS in CMIP5 were evaluated.

Keywords: SNA; Field measurement; Model simulation; China.

INTRODUCTION

Atmospheric particles are complex and consist of all kinds of chemical species which are directly from the natural and anthropogenic emissions or formed as the secondary components (Xu *et al.*, 2012). Sulfate, nitrate and ammonium (abbreviated as SNA) are the dominant secondary species of aerosols (~30–50% in $PM_{2.5}$). They can determine the chemical characteristic of particle by changing particles' hygroscopicity and acidity, influence the optical properties of particles and the earth's radiation balance by scattering and absorbing solar radiation, change cloud nucleation process by acting as cloud condensation nuclei (CCN) and then affect climate, and the most important, penetrate deeply to human lung and deteriorate human health (Xu *et al.*, 2002; Sun *et al.*, 2004; Cheung *et al.*, 2005; Hu *et al.*, 2008; Pathak *et al.*, 2009; Cheng *et al.*, 2011; Sang *et al.*, 2011; Gao *et al.*, 2012; Yan *et al.*, 2012).

Particle pollution is an increasing concerned issue in current China. SNA have a high loading in the atmospheric particle (See section *Contributions to particles*) and play a crucial role on the deteriorated air quality, e.g., in the increasing haze formation in the country (Tan *et al.*, 2009; Du *et al.*, 2011; Huang *et al.*, 2011; Zhang *et al.*, 2012c). As the dominant species, SNA have been widely investigated in many regions in recent years, including various urban and suburban/rural sites as shown in Tables S1 and S2, and a lot of SNA characteristics have been gained. However, most of these researches are associated with the specific SNA levels, formation and sources at specific locations. Few are related to the SNA's characteristics in a national scale. Some studies have paid attention to the description of SNA over the country, but they were usually limited to the model simulation (Wang *et al.*, 2003; Li *et al.*, 2010b). Therefore, up to now, the nationwide SNA pollution characteristic from the ground observation is still blank.

In this study, we investigated the levels, formations and sources, and inter-relationships of SNA across the country based on published data in the field measurements before 2012. To our knowledge, this is the first time for such wide and systematic inspection on SNA in China. This may give a holistic understanding of SNA pollution and benefit the further control. Besides, a model simulation was performed

* Corresponding author.
Tel.: +0086-531-88364896; Fax: +0086-531-88361990
E-mail address: xuehuazhou@sdu.edu.cn (Xuehua Zhou)
bingchen@sdu.edu.cn (Bing Chen)

and the results were evaluated based on the observations, which provides an insight into differentiating the observation and model simulation and is helpful in the evaluation of SNA's radiative forcing in China.

METHODS

Database

There are 226 sets of data about SNA in $PM_{2.5}$ and 88 sets in PM_{10} shown in Tables S1 and S2, which are collected from almost all published literatures before 2012 in the field measurements. These data span from 1997 to 2010 with long term (i.e., annual) and short term (i.e., daily and weekly) averaged concentrations. They are measured at various sites, including urban (i.e., commercial, traffics, industrial and residential sites) and suburban/rural areas (including suburban, rural, park, background, mountain, forest and remote sites). Data with only species without PM mass concentrations or with PM mass without any species concentration in a set (e.g., with PM, SO_4^{2-} and NO_3^- without NH_4^+) are not collected, which guarantees the internal consistency of a data set and a minimum of quality control. Northern and southern China are divided by a demarcation line, Qinling Mountains-Huaihe River Line (Gao *et al.*, 2011a) (see supplementary). There are 103 sets of data in $PM_{2.5}$ in 13 regions of northern China and 123 sets in 18 areas of southern China. In this study, northern and southern China usually refer to aforementioned designation, unless otherwise specified.

Model Simulation

To evaluate the climate model prediction of aerosols in China, we retrieved aerosol concentrations during 2000–2012 from the Goddard Institute for Space Studies (GISS) atmospheric general circulation model (GCM, Model E2 version) in Coupled Model Intercomparison Project Phase 5 (CMIP5) (Hansen *et al.*, 2002a, b; Schmidt *et al.*, 2006; Schmidt *et al.*, 2014). The GISS_E2 simulation has a resolution of 2° × 2.5° latitude by longitude in horizontal and vertically spans 40 layers with top at 0.1 hPa. The simulation included interactive chemistry, aerosols, and dust driven by emissions (Koch *et al.*, 2011), The descriptions of the tracer code, chemical reactions, species, and model evaluation are detailed in the literatures (Shindell *et al.*, 2006, 2013).

Representativeness of the Collected Data

The data in this study from various papers through different techniques at different sites in China over one decade were analyzed based on the supposition that these data accurately represented the characteristics of particles and SNA during sampling time. The comparisons neglected the temporal variations of the data.

Particle concentrations were obtained by gravimetric measurements. The possible systematic errors may come from the different sampler types, various filters (with Teflon, Quartz, Glass fibre filters) (see Tables S1 and S2) and the relative humidity when weighting the samples before and after sampling. The sampler types usually cause a little error since the filtration devices (including sampling heads) were equivalent to reference methods in the published literatures. The inert filters may result in the variable reduction of NH_4NO_3 at different temperature. When the temperature is over 20°C. the losses of NH_4NO_3 can reach 100% from quartz fibre filters (Hering and Cass, 1999; Schaap *et al.*, 2004). This, combined with both negative and positive artefacts for organic matter in particles (Eatough *et al.*, 1993, 1996), may rise the errors of particle mass concentrations. Notably. the losses of NH_4NO_3 during sampling can affect greatly the seasonal variation of NO_3^-, which will be pointed out in the next discussion when the artefacts may influence the conclusions. There were small errors (< 10%) from the different relative humidity through gravimetric measurements (Putaud *et al.*, 2004), so it is negligible in the following discussion.

In the SNA analysis, we considered the accuracy and consistency of analytical techniques, turning out all SNA in our referenced papers were analyzed by ion chromatograph (IC). According to (Putaud *et al.*, 2000), the results from different laboratories are usually within ± 10% for SNA.

RESULTS AND DISCUSSION

Concentration Levels

General Concentrations of SNA in China

The concentrations of SNA in $PM_{2.5}$ are shown in Table S1. From the table, the average concentrations of SNA are 17.96 ± 10.23 (2.17 to 60.90 μg m^{-3}), 7.66 ± 5.68 (0.13–35.60 μg m^{-3}) and 7.26 ± 5.11 μg m^{-3} (0.10–29.80 μg m^{-3}), respectively. These are about 3–5 times greater than those in USA (2.84, 1.78 and 1.58 μg m^{-3} for SNA in $PM_{2.5}$, respectively) (Hand *et al.*, 2011) and Europe (4.37, 1.75 and 1.54 μg m^{-3} for SNA in $PM_{2.5}$, respectively). Sillanpää *et al.* (2006) suggesting severer SNA pollutions in China. Such high SNA levels can be attributed to higher precursors emissions, e.g., for sulfate, annual average 22.45 Tg SO_2 emissions in China (China Statistical Yearbook, 2002–2013) was higher than annual average 11.56 Tg SO_2 emissions in USA (during 2001–2012, http://www.epa.gov/ttnchie1/trends) and 6.78 Tg SO_2 emissions in Europe (during 2001–2012, http://www.eea. europa.eu/) when the territory area of China is comparable to USA and about 2 times of Europe Union countries.

Contributions to Particles

Total fractions of SNA in $PM_{2.5}$ and PM_{10} were 34.2 ± 10.9% and 28.2 ± 8.5%, respectively, in the country (Fig. 1). In $PM_{2.5}$, sulfate (19.5 ± 7.6%) contributes more to particles than nitrate (7.3 ± 3.6%) and ammonium (7.3 ± 3.3%). The corresponding fractions of the three species in PM_{10} are 15.6 ± 6.2%, 7.6 ± 3.0% and 5.1 ± 2.4%, respectively. Notably, the fractions of nitrate in $PM_{2.5}$ and PM_{10} are comparable. Considering that the mass concentration of PM_{10} is higher than that of $PM_{2.5}$ (175.28 ± 118.94 μg m^{-3} vs. 99.63 ± 54.69 μg m^{-3} in Tables S2 and S1), this signifies that nitrate in coarse particles has a certain contribution to PM_{10} mass and can't be ignored (Li *et al.*, 2008; Yan *et al.*, 2012), which is consistent with the results from Putaud *et al.* (2004) in Europe.

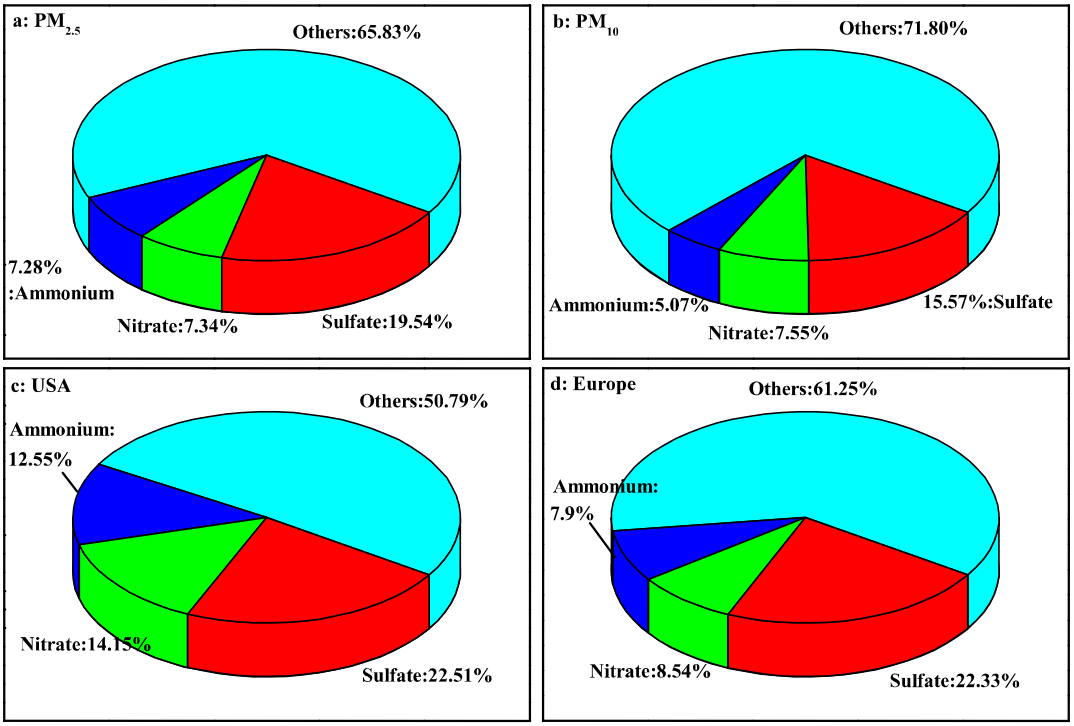

Fig. 1. The fractions of sulfate, nitrate and ammonium in (a) $PM_{2.5}$ and (b) PM_{10} of China, in $PM_{2.5}$ of (c) USA and (d) Europe, respectively.

Compared to those in USA (49.2%) (Hand *et al.*, 2011) and Europe (38.7%) (Sillanpää *et al.*, 2006), the total SNA fraction in fine particle in China is lower (Figs. 1(a), 2(c) and 2(d)). The contributions of each SNA species to fine particle in China are lightly lower than those in Europe (Sillanpää *et al.*, 2006). However, the proportion of sulfate in China is near that in USA (Hand *et al.*, 2011) and nitrate and ammonium are about a half of those in USA (Hand *et al.*, 2011).

Spatial and Temporal Distributions

Seasonal Distributions

From Table 1, the concentration trends of SNA in China are winter > summer > autumn > spring, winter > autumn > spring > summer, winter > autumn > summer > spring, respectively. Peak concentrations occur consistently in winter for SNA in China, but the lowest values are in spring for sulfate and ammonium and in summer for nitrate, which are attributed to the distinct climate and source emissions. The high sulfate concentration in winter may be attributed to the heavy SO_2 emissions and primary sulfate emissions (see Section *Formation of sulfate and nitrate aerosols from gaseous precursor conversion*), e.g., the increasing emissions from the extra coal burning for heating in the northern China, which also resulted in the highest sulfate concentration in the cold season in the north. The low rate of removal via less wet deposition in this season as shown in Table 2 is also an important factor to contribute higher sulfate level. In summer and autumn, the temperature and RH are relative high (Table 2), and there are higher SO_2 emissions in late autumn, which will activate the photochemical reactions and result in higher sulfate concentrations in the two seasons (Hu *et al.*, 2002; Sun *et al.*, 2004). In comparison, in spring, RH and temperature are lower (Table 2) and there are more violent winds, which can inhibit the formation of sulfate (Yang *et al.*, 2007). In northern China, sulfate adopts the same pattern as the whole country. While in southern China, the level of sulfate in autumn is comparable to that in winter and higher than that in summer, which is different from that in northern China with the lower value in autumn than those in winter and summer. This may be attributed to the absence of both the pronounced SO_2 emissions from extra coal combustion in winter and obviously higher temperature in summer than in autumn in the south.

Table 1. The average concentration of SNA in four seasons in China, North and South in China.

μg m^{-3}	Average			North			South		
	SO_4^{2-}	NO_3^-	NH_4^+	SO_4^{2-}	NO_3^-	NH_4^+	SO_4^{2-}	NO_3^-	NH_4^+
Spring	13.94	6.63	5.29	15.07	7.59	5.41	12.48	5.39	5.13
Summer	17.48	4.81	5.60	20.90	6.59	7.53	14.36	3.18	3.85
Autumn	16.70	7.36	7.51	16.64	7.82	6.99	16.74	6.98	7.94
Winter	21.91	11.96	10.05	26.75	14.68	12.53	16.74	9.06	7.40

Table 2. The emissions of SO_2 and NO_x in four seasons of China; the average wet precipitation, rainfall frequency in four seasons of China; the average RH and temperature in northern and southern China.

	SO_2 (Gg)[a]	NO_x (Gg)[a]	Average rainfall frequency/Days[b]	The average total wet precipitation/mm[c]			RH/%[c]			T/°C[c]		
				Average	North	South	Average	North	South	Average	North	South
Spring	7385	5028	12	68.69	29.30	110.22	58.00	44.45	69.98	14.95	11.80	18.30
Summer	7387	4996	12	142.80	97.30	191.12	68.60	61.56	75.90	25.15	23.20	26.80
Autumn	7757	5230	10	67.19	39.05	94.80	67.68	61.56	74.40	14.97	11.70	20.30
Winter	8489	5576	6	26.93	7.01	43.38	61.97	52.71	72.36	1.92	–2.90	10.10

[a] Zhang *et al.* (2009a).
[b] http://www.tianqi.com/.
[c] China Statistical Yearbook (2002–2013).

Nitrate exhibits an obvious seasonal variation with the highest level in winter and the lowest in summer in northern China, southern China and the whole country. It should be pointed out that the losses of NH_4NO_3 are huge during the sampling and may reach 100% from quartz fibre filters in summer (Hering and Cass, 1999; Schaap *et al.*, 2004). When we multiply the measured nitrate concentrations in summer by 2 to reevaluate its pattern in season, it is found that even so, the nitrate levels in winter are still the highest in northern China, southern China and the whole country. It is well known that nitrate concentration is affected by NO_2 emissions and the meteorological factors (such as temperature). NO_2 is mainly from the vehicular emissions and coal burning emissions. Due to the almost even distribution of traffic emissions over the year round, the variations of nitrate may be strongly associated with the coal burning and the meteorological factors (Wang *et al.*, 2006b; Zhang *et al.*, 2009b). In the whole country, NO_x emissions are slight higher in winter than those in other three seasons due to the extra emissions from coal burning for heating in northern China. The relative high NO_x emissions, the less wet precipitation and favorable shift from gas phase to particle phase as a result of lower temperature in winter jointly lead to high nitrate concentration. In summer, NO_x emissions are relative low and temperature is high, which benefits the conversion of gaseous NO_2 to HNO_3, but is adverse for gaseous HNO_3 to particulate nitrate. These, combined with high wet precipitation, probably result in the low nitrate concentration. It should be pointed out that the artefacts from the volatilization of NH_4NO_3 on the filter during the sampling in summer should also have a significant contribution to the lower nitrate concentration. In northern China, in winter, NO_x emissions are heavier due to the heating (Table 1), which, combined with the low temperature, which is favorable for the shift from gaseous HNO_3 to particulate nitrate, causes the high nitrate concentration (Yang *et al.*, 2007). In comparison, in southern China, the higher nitrate concentration in winter may be attributed to lower temperature and less wet precipitation than other seasons (Table 2). In summer, whether northern or southern China, the same reasons as above mentioned result in the lowest nitrate concentrations.

The seasonal pattern of ammonium resembles sulfate with the highest concentration in winter in the country due to the preferred reaction of NH_3 with H_2SO_4 more than with HNO_3 (Tang *et al.*, 2004). The conversion of NH_3 to ammonium aerosol relies on the concentrations of sulfate and nitrate in the atmosphere, temperature and available water, as well as the NH_3 level (Zhang *et al.*, 2011). In winter, the more neutralization reactions of NH_3 with SO_2 and NO_x, lower temperature and higher acidic species favor the shift from the NH_3 (g) to $(NH_4)_2SO_4$ (s) and NH_4NO_3 (s) (He *et al.*, 2001; Wang *et al.*, 2006a; Qu *et al.*, 2008). In contrast, the higher temperature in summer is unfavorable for the conversion of NH_3 to ammonium aerosol. Meanwhile, the sampling artifact from the NH_4NO_3 composition on quartz fibre filter at relative high temperature should also have a certain contribution to the relative low ammonium concentration. In northern China, the ammonium follow completely the seasonal pattern of sulfate in the region. While in southern China, ammonium levels in autumn and winter are higher than those in spring and summer. The significant low concentration in summer is probably related to the losses of NH_4NO_3 in the sampling and the shift of particulate ammonium to gas NH_3.

Spatial Distributions

Fig. 2 exhibits spatial variations of sulfates, nitrates and ammonium in $PM_{2.5}$. From the figure, high SNA concentrations occur in North China Plain (e.g., Beijing), Yangtze River delta (e.g., Shanghai) and Sichuan Basin (e.g., Chongqing), which is in accord with the results from Wang *et al.* (2013) and Li *et al.* (2010b). This is probably related to their higher precursors emissions derived from the extra coal consumption for collective heating in cold season in northern China, rapid economic development and high population density in Yangtze River delta and the terrain unfavorable for the air diffusion in Sichuan Basin. Low SNA levels are observed at sparsely populated mountain, forest and background sites, such as Jianfengling (Li *et al.*, 2010a), Mt. Tai (Deng *et al.*, 2010) and Hok Tusi (Lai *et al.*, 2007). The maxima in urban are 60.90, 35.60 and 29.80 μg m^{-3} for SNA, respectively, may reach 28, 274 and 298 times of the minima at mountain, forest and background sites, suggesting a vast inhomogeneity in the distribution.

Besides this, the SNA distributions in $PM_{2.5}$ in urban and rural areas are also different. SNA show the highest concentrations in urban sites with the averages of 19.83, 8.70 and 8.03 μg m^{-3}, then slightly low levels in suburban sites with the mean values of 14.25, 5.97 and 5.46 μg m^{-3},

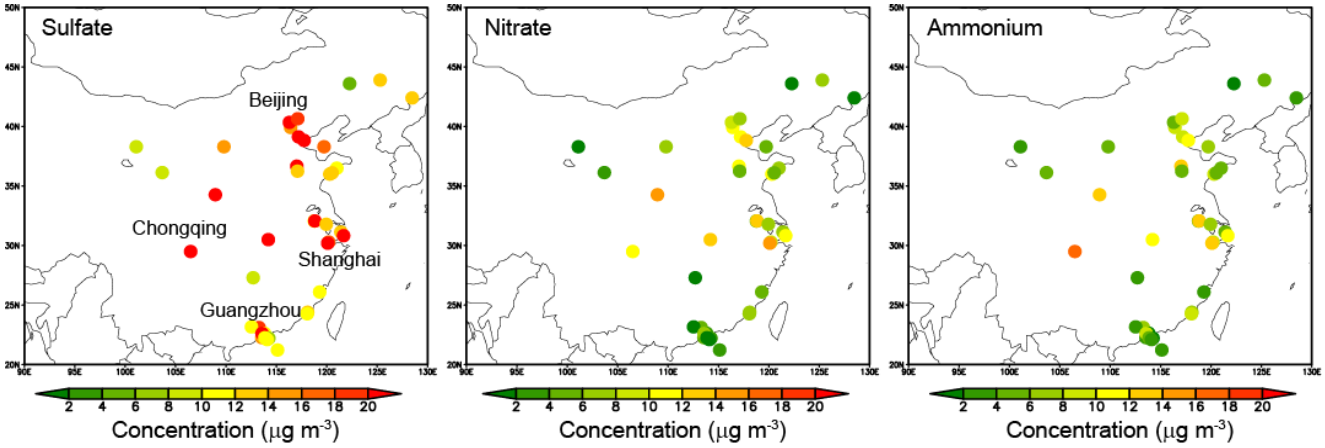

Fig. 2. Annual mean concentrations of sulfates, nitrates, and ammonium in $PM_{2.5}$.

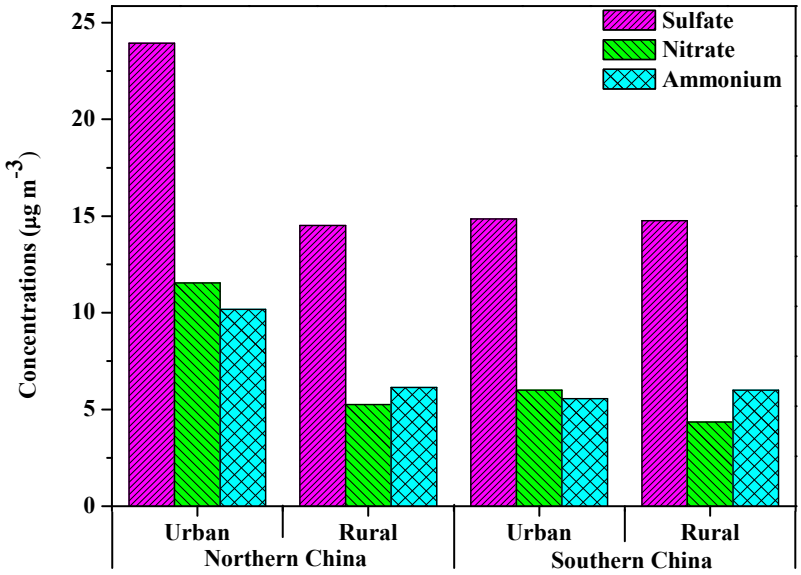

Fig. 3. The spatial distributions of sulfate, nitrate and ammonium in $PM_{2.5}$ in the urban and rural areas of northern and southern China.

which are comparable with those (15.01, 5.44 and 6.52 μg m^{-3} for SNA, respectively) in rural sites. The lowest SNA concentrations occur in background sites with the percentages of 59.7% (11.84 μg m^{-3}), 37.6% (3.27 μg m^{-3}) and 47.7% (3.83 μg m^{-3}) of SNA in urban areas. Fig. 3 shows SNA patterns in $PM_{2.5}$ in urban and rural areas (including suburban, rural, background, mountain, and forest sites in Table S1) in northern and southern China. Obviously, SNA are higher in northern China, especially the urban areas, than those in southern China. This may be contributed two reasons: firstly, the emissions of precursors of SO_2 and NO_x in the north are much higher than that in the south (e.g., 12.40 Tg in the north versus 9.28 Tg in the south for SO_2 emissions and 13.50 Tg in the north versus 10.22 Tg in the south for NO_x emissions) (China Statistical Yearbook, 2002–2013) due to more heavy industries and collective heating in winter in the north; secondly, the subtropical high pressures, typhoon, heavy monsoon rain (e.g., the annual average wet precipitation: 7995.4 mm in the north versus 18693.1 mm in the south (China Statistical Yearbook, 2002–2013) in the south favor the removal and dispersion of SNA. In the comparisons between urban and rural areas, it is found that SNA concentrations are higher in urban than those in rural areas in northern China. This may be attributed to more emissions of industry, vehicle exhaust and construction activities caused by dense residents in cities to elevate SNA levels (Sun *et al.*, 2004; Wang *et al.*, 2009; He *et al.*, 2011; Zhang *et al.*, 2012c). While in the south, the SNA levels are comparable between in urban and rural areas. This is probably due to the consistency of emission sources and/or the transportations of pollutants from urban to suburban/rural sites.

Formations and Sources

Formation of Sulfate and Nitrate Aerosols from Gaseous Precursor Conversion

It is well known that sulfate can be produced in the atmosphere by two ways: gaseous phase oxidation and

aqueous phase reaction. In the gaseous phase, SO_2 can react with OH radical followed by condensation of H_2SO_4 to form sulfate. In comparison, the aqueous phase reaction is more important due to forming the majority of sulfate in most circumstances (Langner and Rodhe, 1991; Guo *et al.*, 2012; Harris *et al.*, 2013), which includes the oxidation of SO_2 with H_2O_2/O_3 and transition metal in cloud and fog droplets and the heterogeneous reactions of SO_2 on aerosol surfaces (Deng *et al.*, 2010). Sulfur oxidation ratio (SOR), which is defined as $S_{nss\text{-}SO4}^{2-}/(S_{nss\text{-}SO4}^{2-} + S_{SO2})$, is a measure of the oxidation degree of sulfur. When SOR is smaller than 0.10, sulfate can be considered from the primary emissions, otherwise, it is produced through the oxidation of SO_2 (Wang *et al.*, 2011). Similarly, nitrate is generally produced by the oxidation of nitrogen oxides and then reacts with NH_3 via homogeneous and heterogeneous reactions (Zheng *et al.*, 2008; Ye and Chen, 2009; Zhang *et al.*, 2009b; Ma *et al.*, 2011; Lei and Wuebbles, 2013). Apart from the photochemical oxidation of NO_x to HNO_3, the formation of nitrate in particle is also influenced by the temperature dependent equilibrium between gaseous phase HNO_3 and particulate nitrate: $NH_3(g) + HNO_3(g) \leftrightarrow NH_4NO_3(s)$ (Zhou *et al.*, 2009). Nitrogen oxidation ratio (NOR), which is defined as $N_{NO3}/(N_{NO3} + N_{NO2})$, is usually used to express the oxidation degree of nitrogen (Zhang *et al.*, 2011). Higher SOR and NOR values suggest more secondary aerosols produced by oxidation of gaseous species in the atmosphere.

SOR and NOR values are calculated in this investigation based on almost all published literatures before 2012 with four seasons as shown in Table 3. From the table, in northern China, SOR is significantly larger in summer than those in other three seasons. The gaseous phase oxidation of SO_2 to sulfate by OH radical has a strong dependence on temperature (Wang *et al.*, 2006b); while high RH favors the aqueous heterogeneous formation of sulfate. In summer, both temperature and RH are high (Table 2), which may enhance the formation of sulfate by gaseous and aqueous phase reactions, so there are relative high SOR values. In winter, the SOR values are lower, even less than 0.1 in some areas, suggesting the conversions of SO_2 to sulfate through neither gas nor aqueous phase are active in the low temperature, and primary emissions from coal combustion become the principal sources. In southern China, the SOR values are comparable in four seasons with all larger than 0.1 (Wang *et al.*, 2006b; Xu *et al.*, 2012; Zhang *et al.*, 2012a), suggesting SO_2 has active photochemical reactions in the atmosphere. Considering that when RH is larger than 75%, sulfate is largely from heterogeneous reactions of photochemical oxidation (Wang *et al.*, 2006b), the average RH of 69.98–75.90% in southern China (Table 2) means the enhancement of sulfate formation is probably more related to heterogeneous reactions. The comparable SOR in four seasons may be attributed to the warm and humid weather throughout the whole year in the region.

NOR values are lower than SOR values (Table 3). NOR values are the highest in summer or in winter in Beijing (Wang *et al.*, 2005; Deng *et al.*, 2011) and Ji'nan (Gao *et al.*, 2011b) of northern China, suggesting that in different samplings, either the oxidization of NO_x to HNO_3, e.g., in summer, or the equilibrium between gaseous phase HNO_3 and particulate nitrate, e.g., in winter, determines the particulate nitrate formation. In contrast, in the two cities of southern China, Xiamen (Zhang *et al.*, 2012a) and Fuzhou (Xu *et al.*, 2012), the highest NOR values occur in winter, meaning the equilibrium between gaseous phase HNO_3 and particulate nitrate is dominated in the particulate nitrate formation. The high temperature and RH in summer are favorable for the conversion of NO_x to HNO_3, but also promote the shift of NH_4NO_3 from particulate phase to gaseous phase. Moreover, the higher the temperature is, the larger amount H_2SO_4 produced from SO_2 oxidation, which competes with HNO_3 for NH_3, slowing the production of nitrate. These, along with the emissions of NO_x (Table 2), determine the formation of nitrate in the particulate phase is higher in summer or winter in northern China and in winter in southern China. Notably, the artefacts from the losses of NH_4NO_3 in the sampling in summer can reduce the NOR values and probably have a significant effect on the season trends of NOR.

The Main Sources, Coal Combustion or Vehicle Exhaust Emissions?

The mass ratio of nitrate to sulfate has been used as a tracer for the relative importance of mobile vs. stationary sources of nitrogen and sulfur in the atmosphere (Wang *et al.*, 2005; Lai *et al.*, 2007; Shen *et al.*, 2007; Cao *et al.*, 2009; Li *et al.*, 2009). It has been indicated that high nitrate to sulfate ratios will be observed when the influences of vehicular emissions surpass those from the coal combustion emissions (Yang *et al.*, 2011). In China, the estimated NO_x to SO_x ratios from gasoline burning, diesel burning, and coal combustion are 13:1, 8:1 and 1:2 (Yao *et al.*, 2002; Wang *et al.*, 2005), respectively, thus it is reasonable to use nitrate and sulfate as the indicators of mobile and stationary emissions, respectively.

The mass ratios of NO_3^-/SO_4^{2-} are 0.03–2.14 with an average of 0.43 ± 0.26 in China, which is lower than those in America (0.63) (Hand *et al.*, 2011) and comparable to Europe (0.47) (Sillanpää *et al.*, 2006). The ratio is less than 1 and suggests that stationary sources (coal combustions) are still dominated in the country (Lai *et al.*, 2007; Li *et al.*, 2009). In order to examine the seasonal patterns of NO_3^-/SO_4^{2-} ratios, the measurements with all four seasons were selected from Table S1 as shown in Table 4. There are obvious seasonal variations for the ratios with much lower in summer and higher in winter and spring. This may be attributed to the high temperatures, RH and radiations in summer, which are favorable for the formation of sulfate, but not for the formation of $NH_4NO_3(s)$, which is apt to decomposing in the high temperature. In addition, the NH_4NO_3 composition on quartz filter during the sampling also should have a non-ignorable contribution to lower NO_3^-/SO_4^{2-} ratios. In early spring and winter, the low temperature favors a shift from the gaseous phase as HNO_3 to the particulate phase as NH_4NO_3, but against for sulfate (see Section *Formation of sulfate and nitrate aerosols from gaseous precursor conversion*), which results in higher NO_3^-/SO_4^{2-} ratios in the two seasons, even more than one in part areas (Duan *et al.*, 2006; Yang *et al.*, 2007; Yang *et al.*, 2011).

Table 3. The SOR and NOR in four seasons in China.

	Locations	Times	Spring	Summer	Autumn	Winter	References
SOR	Beijing1	Aug. 2001–Sep. 2002	0.16	0.35	0.27	0.05	(Duan *et al.*, 2006)
	Beijing2	Jul. 2008–Apr. 2009	0.23	0.62	0.49	0.13	(Deng *et al.*, 2011)
	Beijing3	2001–2003	0.12	0.39	0.19	0.17	(Wang *et al.*, 2005)
	Jinan1	Dec.2007–Oct. 2008	0.22	0.47	0.30	0.17	(Gao *et al.*, 2011b)
	Jinan2	Mar. 2006–Feb. 2007	0.38	0.62	0.41	0.18	(Yang *et al.*, 2012)
			0.23	0.49	0.24	0.10	
	Xiamen	Jun. 2009–May. 2010	0.25	0.22	0.22	0.29	(Zhang *et al.*, 2012a)
	Fujian	Apr. 2007–Jan. 2008	0.18	0.23	0.26	0.24	(Xu *et al.*, 2012)
NOR	Beijing1	Aug. 2001–Sep. 2002	0.06	0.08	0.09	0.11	(Duan *et al.*, 2006)
	Beijing2	Jul. 2008–Apr. 2009	0.17	0.30	0.20	0.10	(Deng *et al.*, 2011)
	Beijing3	2001–2003	0.05	0.08	0.04	0.05	(Wang *et al.*, 2005)
	Jinan	Dec. 2007–Oct. 2008	0.14	0.28	0.14	0.12	(Gao *et al.*, 2011b)
	Xiamen	Jun. 2009–May. 2010	0.07	0.06	0.07	0.10	(Zhang *et al.*, 2012a)
	Fujian	Apr. 2007–Jan. 2008	0.05	0.02	0.04	0.10	(Xu *et al.*, 2012)

Table 4. The mass ratios of NO_3^-/SO_4^{2-} in $PM_{2.5}$ in four seasons in China.

Locations	Times	Spring	Summer	Autumn	Winter	References
Beijing 1	Jul. 1999–Sep. 2000	0.72	0.27	0.89	0.62	(He *et al.*, 2001)
Beijing 2	Aug. 2001–Sep. 2002	0.69	0.40	0.85	1.09	(Duan *et al.*, 2006)
Beijing 3	2001–2003	0.88	0.61	0.72	0.59	(Wang *et al.*, 2005)
Jinan 1	Nov. 2004–Sep. 2005	0.57	0.11	0.30	1.09	(Yang *et al.*, 2007)
Jinan 2	Mar. 2006–Feb. 2007	0.41	0.18	0.33	0.53	(Yang *et al.*, 2012)
		0.47	0.07	0.29	0.53	
Qingdao	1997–2000	0.28	0.21	0.26	0.56	(Hu *et al.*, 2002)
Hangzhou	Apr. 2004–Mar. 2005	0.40	0.25	0.48	0.67	(Liu *et al.*, 2007)
		0.53	0.30	0.45	0.69	
		0.48	0.39	0.53	0.70	
Shanghai 1	May. 1999–Mar. 2000	0.43	0.29	0.38	0.54	(Ye *et al.*, 2003)
Shanghai 2	Sep. 2003–Jan. 2005	0.77	0.48	0.43	0.60	(Wang *et al.*, 2006b)
Fuzhou	Apr. 2007–Jan. 2008	0.45	0.17	0.27	0.59	(Xu *et al.*, 2012)
Xiamen	Jun. 2009–May. 2010	0.65	0.37	0.44	0.50	(Zhang *et al.*, 2012a)
		0.53	0.37	0.49	0.74	
		0.49	0.55	0.47	0.59	

Another meaningful inspection was performed between the correlations of sulfate and nitrate. The mass concentrations of sulfate and nitrate exhibit a relative weak correlation (R^2 = 0.42, p = 0.00) (Fig. 4). However, there is a significantly negative correlation between the mass percentages of sulfate and nitrate when there are high sulfate plus nitrate loadings in $PM_{2.5}$, for example, the proportions of sulfate plus nitrate in $PM_{2.5}$ are ≥ 40% (R^2 = 0.53, p = 0.00) and 30–40% (R^2 = 0.62, p = 0.00) (Fig. 5). It suggests that the results from the former study in Shanghai, Hangzhou and Guangzhou (Kong *et al.*, 2014) are not local phenomena, but a universal rule across the country. The negative correlation signifies that more nitrates will probably be produced when sulfate formation decreases along with the reduction of SO_2 from current emission control strategies. Nitrate aerosol will become more crucial in the future atmosphere along with the increase in nitrogen oxide emissions and probably cause serious air pollution just like that of sulfate in China.

Relationships among Sulfate, Nitrate and Ammonium

In order to explore the existent forms of SNA across China, the correlations of SNA were determined by regression analysis. In Fig. 4, sulfate and ammonium has a good correlation with a correlation coefficient of 0.62 (p = 0.00), implying that they are associated with the same particulate system. In the atmosphere, ammonium is mainly produced by the reaction between gaseous NH_3 and acidic sulfate and nitrate particles (Yang *et al.*, 2005). The molar ratio of sulfate to ammonium for $(NH_4)_2SO_4$ and NH_4HSO_4 are 0.50 and 1.00, respectively. So the sulfate to ammonium slope of 0.28 in Fig. 6 suggests ammonium is rich and sulfate is completely neutralized by ammonium, and $(NH_4)_2SO_4$ are formed in aerosols (Wang *et al.*, 2006b; Li *et al.*, 2009). Moreover, nitrate also shows a good correlation with ammonium (R^2 = 0.66, p = 0.00) with a slope of less than 1, meaning that the formation of NH_4NO_3 and the possible existences of other anions (such as Cl^-, F^-, Br^-, $C_2O_4^{2-}$…) in particles (He *et al.*, 2001; Hu *et al.*, 2002; Yang *et al.*, 2005; Li *et al.*, 2008; Yang *et al.*, 2012). Notably, the regression fitted between ($2[SO_4^{2-}] + [NO_3^-]$) and $[NH_4^+]$ shows a strongly linear correlation with a slope very closely to 1, indicating a completely neutralized system, and $(NH_4)_2SO_4$ and

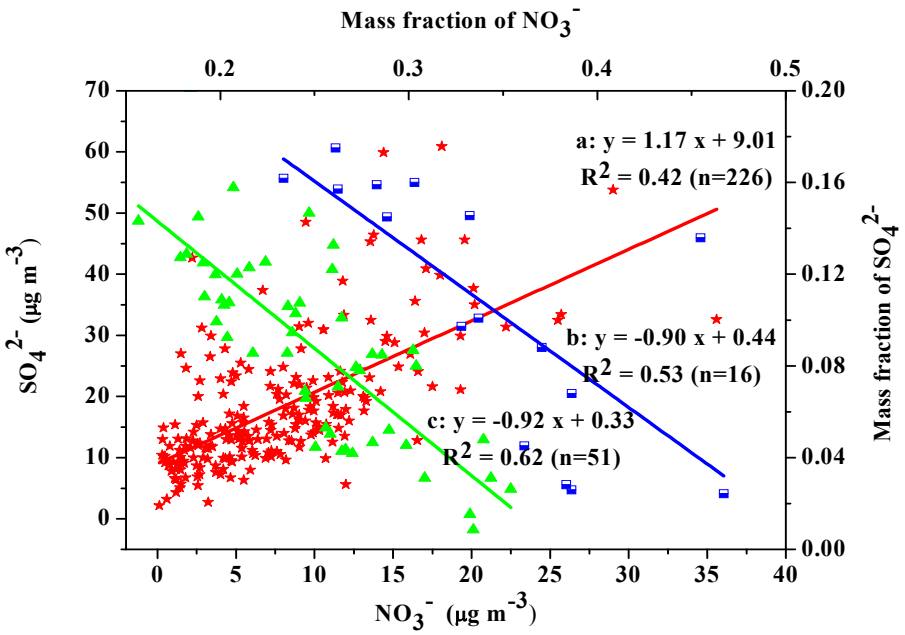

Fig. 4. The relationships of $SO_4^{2-}$and NO_3^- (a), the mass fractions of SO_4^{2-} and NO_3^- when the proportions of sulfate plus nitrate in $PM_{2.5}$ are ≥ 40% (b) and 30−40% (c).

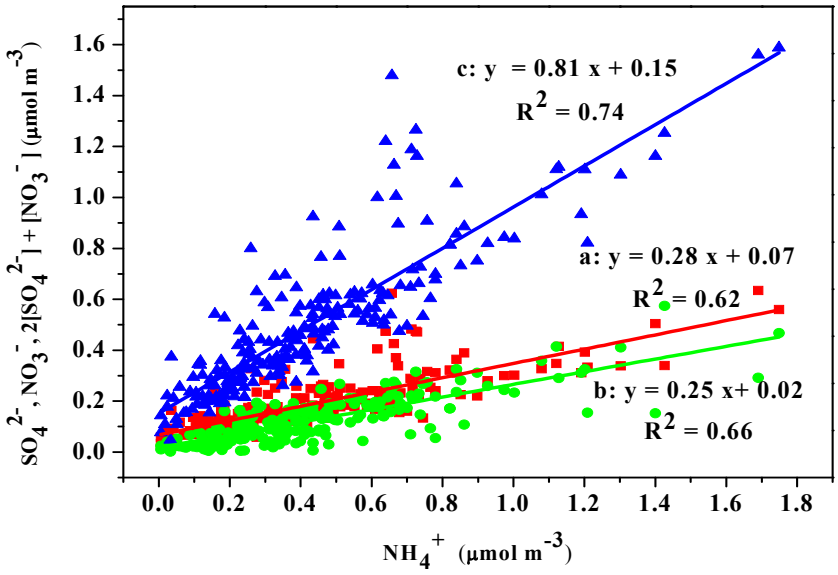

Fig. 5. The relationships of SO_4^{2-} and NH_4^+ (a), NO_3^- and NH_4^+ (b), $2[SO_4^{2-}] + [NO_3^-]$ and NH_4^+ (c) in $PM_{2.5}$.

NH_4NO_3 may be the major compounds that SNA exist in the atmospheric particles in China.

Evaluation for Climate Model

Climate models are useful to predict aerosol concentrations and radiative forcing, despite considerable uncertainties of simulations in key source regions such as China (Bauer *et al.*, 2007; Han *et al.*, 2011; Zhang *et al.*, 2012b; Cheng *et al.*, 2013). We retrieved data during 2000–2012 from GISS model in CMIP5 to simulate SNA's spatial and temporal distributions. The simulated average SNA by GISS are in good agreements with the observations in spatial patterns as shown in Figs. 6–9. The GISS simulation well captured the winter peaks of nitrate (Fig. 6) and ammonium (Fig. 7), although the ammonium concentration was slightly under-predicted in middle China during winter season. This underestimation of ammonium may be caused by uncertainties of emissions and/or photochemical parameterization in GISS model. However, sulfate concentrations in the model are obvious lower in winter than summer levels, contrasting to the observed maximum sulfate concentration in winter (Fig. 8). The model performed well for the prediction of sulfate during summer, however, sulfate concentration in winter were significant underpredicted in northern China (Fig. 9). Such underprediction of winter sulfate in northern China is also reported in other climate models, such as

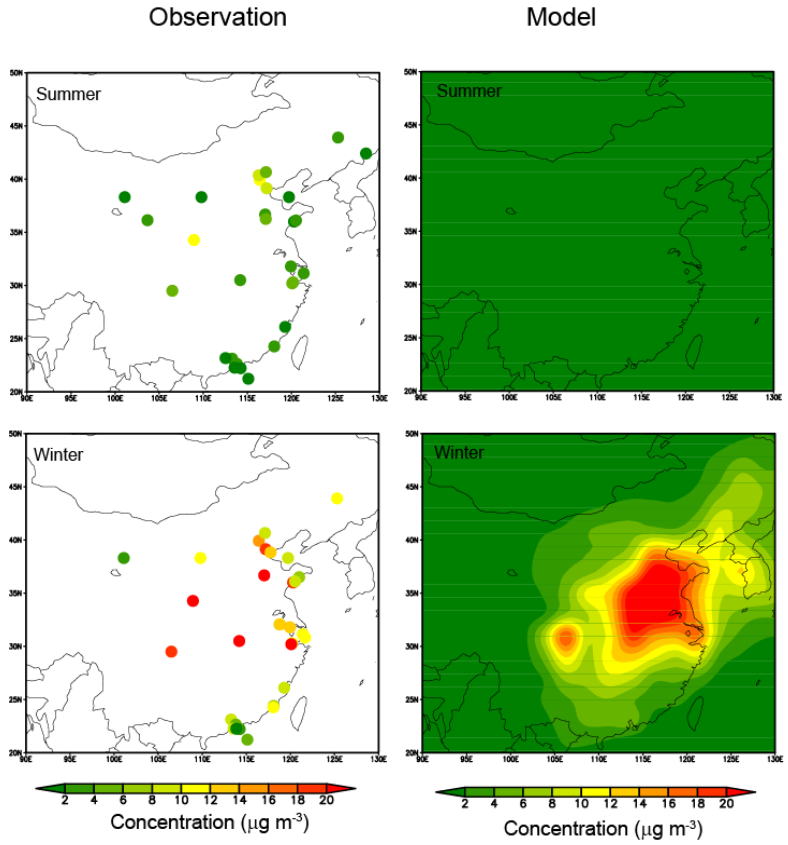

Fig. 6. Nitrate concentrations of observations (left panels) and GISS prediction (right panels).

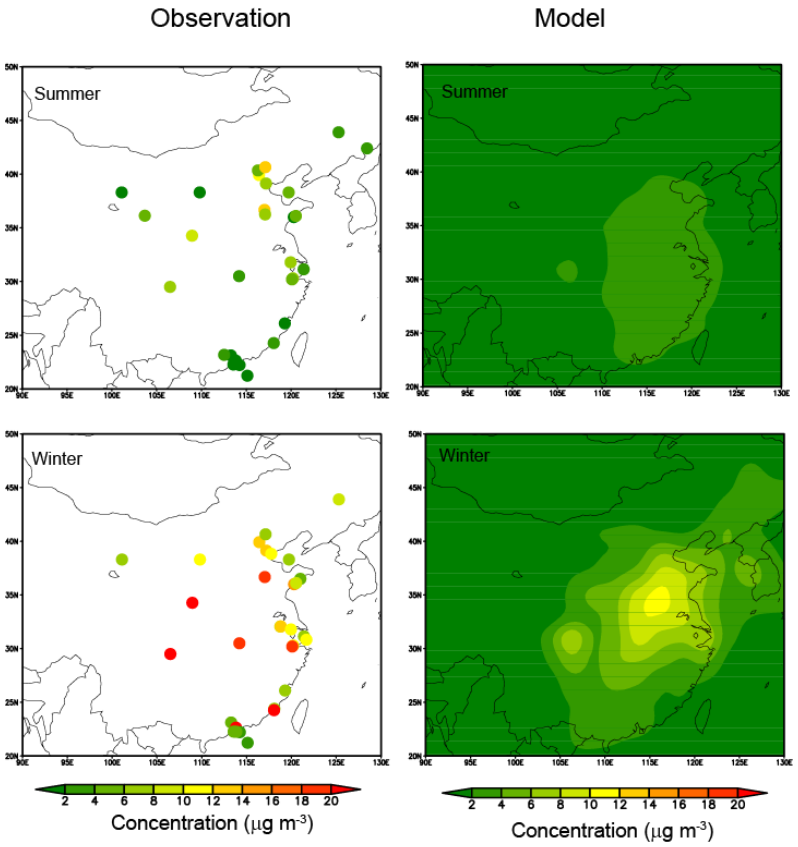

Fig. 7. Ammonium concentrations of observations (left panels) and GISS prediction (right panels).

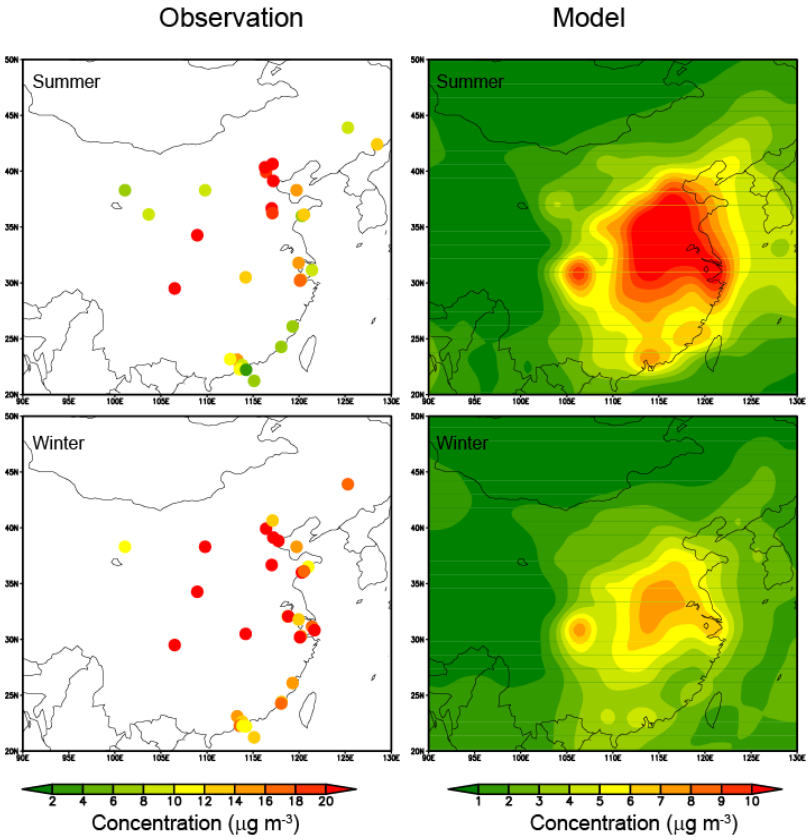

Fig. 8. Sulfate concentrations of observations (left panels) and GISS prediction (right panels).

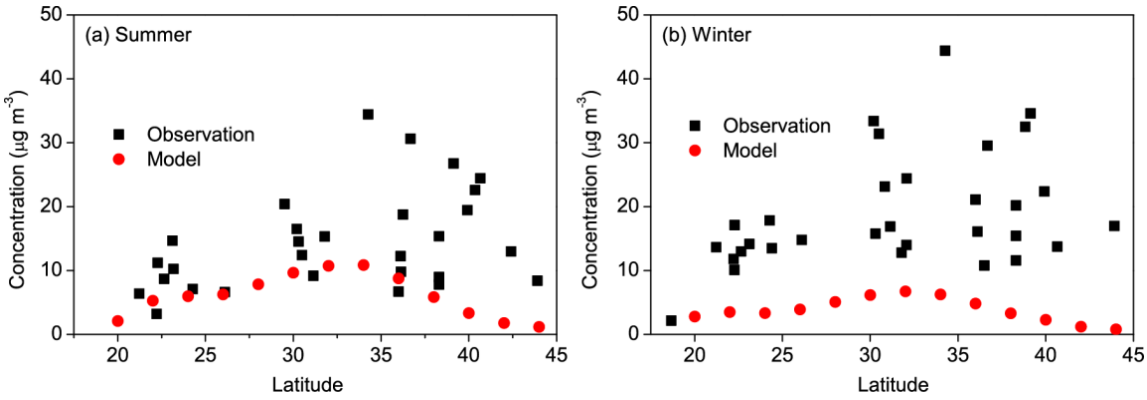

Fig. 9. Comparison between model and observation for latitude trend of sulfate concentrations in summer (a) and winter (b). The model shows the average between 110 to 120° in longitude. Sites of observation are shown in Fig. 8.

GEOS-Chem (Wang *et al.*, 2013) (Fig. S2). This means that although SO_2 emissions in China peak in winter (Table 2), the photochemical production of sulfate probably isn't yet well resolved in the model in the severe polluted area in northern China, such as Northern China Plain (NCP).

CONCLUSIONS

In this paper, we investigate SNA in aerosols in China based on almost all data published before 2012 in the field measurements. The results show that SNA in China are much higher than those in USA and Europe. In fine particles, sulfate is the most abundant species among SNA with the average concentration of 17.96 ± 10.23 μg m^{-3} compared to 7.66 ± 5.68 μg m^{-3} and 7.26 ± 5.10 μg m^{-3} for nitrate and ammonium, respectively. SNA occupy 34.2 ± 10.9% of $PM_{2.5}$ mass and 28.2 ± 8.5% of PM_{10} mass in the country. In the seasonal distribution, SNA all have the highest concentrations in winter, but the lowest levels are in spring for sulfate and ammonium and in summer for nitrate. In the spatial pattern, the high SNA concentrations occur in North China Plain, Yangtze River delta and Sichuan Basin, especially high in the urban areas in North China Plain. The formation of sulfate and nitrate are different in

different regions (e.g., northern and southern China) and seasons. Sources analyses find that the mean NO_3^-/SO_4^{2-} ratio is 0.43 ± 0.26, signifying that stationary sources (coal combustions) are still dominant in China. The regression analysis suggests that $(NH_4)_2SO_4$ and NH_4NO_3 are the main existence forms of SNA in China. On these observations, the model simulation for SNA aerosols are evaluated. The simulation by GISS model in CMIP5 in both summer and winter show good agreement with SNA concentrations based on the observations. However, the simulated sulfate concentrations present the maximum in summer, contrasting to the highest observational concentration in winter when the simulated nitrate and ammonium concentrations are consistent with the observations in seasons, which is probably attributed to the underestimation of sulfate in the model in northern China in winter. These results provide useful information on SNA in China and is significant for the establishment of policy for legislator to reduce particle pollution in the country.

ACKNOWLEDGMENT

The authors acknowledge the support of Shandong Province Natural Science Foundation (ZR2010DQ022), Independent Innovation Foundation of Shandong University (2012TS041), China Postdoctoral Science Foundation funded project (20060400982) and Shandong Postdoctoral Science Innovation Foundation (200601003).

SUPPLEMENTARY MATERIAL

Supplementary data associated with this article can be found in the online version at http://www.aaqr.org.

REFERENCES

Bauer, S.E., Koch, D., Unger, N., Metzger, S.M., Shindell, D.T. and Streets, D.G. (2007). Nitrate aerosols today and in 2030: A global simulation including aerosols and tropospheric ozone. *Atmos. Chem. Phys.* 7: 5043–5059.

Cao, J.J., Shen, Z.X., Chow, J.C., Qi, G.W. and Watson, J.G. (2009). Seasonal variations and sources of mass and chemical composition for PM_{10} aerosol in Hangzhou, China. *Particuology* 7: 161–168.

Cheng, S.Y., Lang, J.L., Zhou, Y., Han, L.H., Wang, G. and Chen, D.S. (2013). A new monitoring-simulation-source apportionment approach for investigating the vehicular emission contribution to the $PM_{2.5}$ pollution in Beijing, China. *Atmos. Environ.* 79: 308–316.

Cheng, Y., He, K.B., Duan, F.K., Zheng, M., Du, Z.Y., Ma, Y.L. and Tan, J.H. (2011). Ambient organic carbon to elemental carbon ratios: Influences of the measurement methods and implications. *Atmos. Environ.* 45: 2060–2066.

Cheung, H.C., Wang, T., Baumann, K. and Guo, H. (2005). Influence of regional pollution outflow on the concentrations of fine particulate matter and visibility in the coastal area of southern China. *Atmos. Environ.* 39: 6463–6474.

China Statistical Yearbook, 2002–2013. http://www.stats.gov.cn/tjsj/ndsj/. (in Chinese).

Deng, C., Zhuang, G., Huang, K., Li, J., Zhang, R., Wang, Q., Liu, T., Sun, Y., Guo, Z. and Fu, J.S. (2010). Chemical characterization of aerosols at the summit of Mountain Tai in Central East China. *Atmos. Chem. Phys.* 11: 7319–7332.

Deng, L.Q., Hong, L.I., Chai, F.H., Lun, X.X., Chen, Y.Z., Wang, F.W. and Run-Xiang, N.I. (2011). The pollution characteristics of the atmospheric fine particles and related gaseous pollutants in the northeastern urban area of Beijing. *China Environ. Sci.* 31: 1064–1070 (in Chinese).

Du, H.H., Kong, L.D., Cheng, T.T., Chen, J.M., Du, J.F., Li, L., Xia, X.G., Leng, C.P. and Huang, G.H. (2011). Insights into summertime haze pollution events over Shanghai based on online water-soluble ionic composition of aerosols. *Atmos. Environ.* 45: 5131–5137.

Duan, F.K., He, K.B., Ma, Y.L., Yang, F.M., Yu, X.C., Cadle, S.H., Chan, T. and Mulawa, P.A. (2006). Concentration and chemical characteristics of $PM_{2.5}$ in Beijing, China: 2001–2002. *Sci. Total Environ.* 355: 264–275.

Gao, H.W., Chen, J., Wang, B., Tan, S.C., Lee, C.M., Yao, X.H., Yan, H. and Shi, J.H. (2011a). A study of air pollution of city clusters. *Atmos. Environ.* 45: 3069–3077.

Gao, X., Xue, L., Wang, X., Wang, T. and Yuan, C. (2012). Aerosol ionic components at Mt. Heng in central southern China: Abundances, size distribution, and impacts of long-range transport. *Sci. Total Environ.* 433: 498–506.

Gao, X.M., Yang, L.X., Cheng, S.H., Gao, R., Yang, Z., Xue, L.K., Shou, Y.P., Wang, J., Wang, X.F., Nie, W., Xu, P.J. and Wang, W.X. (2011b). Semi-continuous measurement of water-soluble ions in $PM_{2.5}$ in Jinan, China: Temporal variations and source apportionments. *Atmos. Environ.* 45: 6048–6056.

Guo, J., Wang, Y., Shen, X., Wang, Z., Lee, T., Wang, X., Li, P., Sun, M., Collett, J.L. and Wang, W. (2012). Characterization of cloud water chemistry at Mount Tai, China: Seasonal variation, anthropogenic impact, and cloud processing. *Atmos. Environ.* 60: 467–476.

Han, X., Zhang, M.G., Han, Z.W., Xin, J.Y. and Liu, X.H. (2011). Simulation of aerosol direct radiative forcing with RAMS-CMAQ in East Asia. *Atmos. Environ.* 45: 6576–6592.

Hand, J.L.A., Copeland, D.E., Day, A.M., Indresand, D.H., Malm, W.C., McDade, C.E., Moore, C.T., Pitchford, M.L., Schichtel, B.A. and Watson, J.G. (2011). Spatial and Seasonal Patterns and Temporal Variability of Haze and its Constituents in the United States: Report V. June 2011. Cooperative Institute for Research in the Atmosphere. IMPROVE program.

Hansen, J., Sato, M., Nazarenko, L., Ruedy, R., Lacis, A., Koch, D., Tegen, I., Hall, T., Shindell, D. and Santer, B. (2002a). Climate forcings in Goddard Institute for Space Studies SI2000 simulations. *J. Geophys. Res.* 107: 4347.

Hansen, J., Sato, M., Nazarenko, L., Ruedy, R., Lacis, A., Koch, D., Tegen, I., Hall, T., Shindell, D., Santer, B., Stone, P., Novakov, T., Thomason, L., Wang, R., Wang, Y., Jacob, D., Hollandsworth, S., Bishop, L., Logan, J.,

Thompson, A., Stolarski, R., Lean, J., Willson, R., Levitus, S., Antonov, J., Rayner, N., Parker, D. and Christy, J. (2002b). Climate forcings in Goddard Institute for Space Studies SI2000 simulations. *J. Geophys. Res.* 107: 4347.

Harris, E., Sinha, B., Pinxteren, D., Tilgner, A., Fomba, K. W., Schneider, J., Roth, A., Gnauk, T., Fahlbusch, B., Mertes, S., Lee, T., Collett, J., Foley, S., Borrmann, S., Hoppe, P. and Herrmann, H. (2013). Enhanced role of transition metal ion catalysis during in-cloud oxidation of SO_2. *Science* 340: 963–979.

He, K., Zhao, Q., Ma, Y., Duan, F., Yang, F., Shi, Z. and Chen, G. (2011). Spatial and seasonal variability of $PM_{2.5}$ acidity at two Chinese megacities: Insights into the formation of secondary inorganic aerosols. *Atmos. Chem. Phys.* 11: 25557–25603.

He, K.B., Yang, F.M., Ma, Y.L., Zhang, Q., Yao, X.H., Chan, C.K., Cadle, S., Chan, T. and Mulawa, P. (2001). The characteristics of $PM_{2.5}$ in Beijing, China. *Atmos. Environ.* 35: 4959–4970.

Hering, S. and Cass, G. (1999). The magnitude of bias in the measurement of $PM_{2.5}$ arising from volatilization of particulate nitrate from Teflon filters. *J. Air Waste Manage. Assoc.* 49: 725–733.

Hu, M., He, L.Y., Zhang, Y.H., Wang, M., Yong, P.K. and Moon, K.C. (2002). Seasonal variation of ionic species in fine particles at Qingdao, China. *Atmos. Environ.* 36: 5853–5859.

Hu, M., Wu, Z.J., Slanina, J., Lin, P., Liu, S. and Zeng, L. M. (2008). Acidic gases, ammonia and water-soluble ions in $PM_{2.5}$ at a coastal site in the Pearl River Delta, China. *Atmos. Environ.* 42: 6310–6320.

Huang, K., Zhuang, G., Lin, Y., Fu, J.S., Wang, Q., Liu, T., Zhang, R., Jiang, Y., Deng, C. and Fu, Q. (2011). Typical types and formation mechanisms of haze in an Eastern Asia megacity, Shanghai. *Atmos. Chem. Phys.* 12: 105–124.

Koch, D., Bauer, S.E., Del Genio, A., Faluvegi, G., McConnell, J.R., Menon, S., Miller, R.L., Rind, D., Ruedy, R., Schmidt, G.A. and Shindell, D. (2011). Coupled aerosol-chemistry-climate twentieth century transient model investigation: Trends in short-lived species and climate responses. *J. Clim.* 24: 2693–2714.

Kong, L.D., Yang, Y.W., Zhang, S.Q., Xi, Z., Du, H.H., Fu, H.B., Zhang, S.C., Cheng, T.T., Xin, Y. and Chen, J.M. (2014). Observations of linear dependence between sulfate and nitrate in atmospheric particles. *J. Geophys. Res.* 119: 341–361.

Lai, S.C., Zou, S. C., Cao, J.J., Lee, S.C. and Kin-Fai, H.O. (2007). Characterizing ionic species in $PM_{2.5}$ and PM_{10} in four Pearl River Delta cities, South China. *J. Environ. Sci.* 19: 939–947.

Langner, J. and Rodhe, H. (1991). A global three-dimensional model of the tropospheric sulfur cycle. *J. Atmos. Chem.* 13: 225–263.

Lei, H. and Wuebbles, D.J. (2013). Chemical competition in nitrate and sulfate formations and its effect on air quality. *Atmos. Environ.* 80: 472–477.

Li, J., Zhuang, G.S., Huang, K., Lin, Y.F., Xu, C. and Yu, S.L. (2008). Characteristics and sources of air-borne particulate in Urumqi, China, the upstream area of Asia dust. *Atmos. Environ.* 42: 776–787.

Li, L., Wu, W., Feng, J.L., Zhang, D.P., Li, H.J., Gu, Z.P., Wang, B.J., Sheng, G.Y. and Fu, J.M. (2010a). Composition, source, mass closure of $PM_{2.5}$ aerosols for four forests in eastern China. *J. Environ. Sci.* 22: 405–412.

Li, W.F., Bai, Z.P., Liu, A.X., Chen, J. and Chen, L. (2009). Characteristics of major $PM_{2.5}$ components during winter in Tianjin, China. *Aerosol Air Qual. Res.* 9: 105–119.

Li, W.F., Bai, Z.P., Shi, J.W. and Liu, A.X. (2010b). Pollution characteristics and sources of fine particulate matter in ambient air in Tianjin City. *Res. Environ. Sci.* 23: 394–400.

Liu, G., Teng, W. L., Liu, W.Y., Wang, X.F. and Wang, J. (2007). Pollution levels and water-soluble ions of $PM_{2.5}$ in atmosphere in Hangzhou. *Chin. J. Health Lab. Technol.* 3: 407–418 (in Chinese).

Ma, J.Z., Liu, Y.C., Ma, Q.X., Liu, C. and He, H. (2011). Atmospheric heterogeneous reactions and their environmental effects. *Environ. Chem.* 30: 97–118.

Pathak, R.K., Wu, W.S. and Wang, T. (2009). Summertime $PM_{2.5}$ ionic species in four major cities of China: Nitrate formation in an ammonia-deficient atmosphere. *Atmos. Chem. Phys.* 9: 1711–1722.

Putaud, J.P., Van Dingenen, R., Mangoni, M., Virkkula, A., Raes, F., Maring, H., Prospero, J.M., Swietlicki, E., Berg, O.H. and Hillamo, R. (2000). Chemical mass closure and assessment of the origin of the submicron aerosol in the marine boundary layer and the free troposphere at Tenerife during ACE-2. *Tellus Ser. B* 52: 141–168.

Putaud, J.P., Raes, F., Van Dingenen, R., Brüggemann, E., Facchini, M.C., Decesari, S., Fuzzi, S., Gehrig, R., Hüglin, C., Laj, P., Lorbeer, G., Maenhaut, W., Mihalopoulos, N., Muller, K., Querol, X., Rodriguez, S., Schneider, J., Spindler, G., Brink, H., Tørseth, K. and Wiedensohler, A. (2004). A European aerosol phenomenology-2: chemical characteristics of particulate matter at kerbside, urban, rural and background sites in Europe. *Atmos. Environ.* 38: 2579–2595.

Qu, W.J., Zhang, X.Y., Arimoto, R., Wang, D., Wang, Y. Q., Yan, L. W. and Li, Y. (2008). Chemical composition of the background aerosol at two sites in southwestern and northwestern China: potential influences of regional transport. *Tellus Ser. B* 60: 657–673.

Sang, X.F., Chan, C.Y., Engling, G., Chan, L.Y., Wang, X. M., Zhang, Y.N., Shi, S., Zhang, Z.S., Zhang, T. and Ming, H.U. (2011). Levoglucosan enhancement in ambient aerosol during springtime transport events of biomass burning smoke to Southeast China. *Tellus Ser. B* 63: 129–139.

Schaap, M., Spindler, G., Schulz, M., Acker, K., Maenhaut, W., Berner, A., Wieprecht, W., Streit, N., Müller, K. and Brüggemann, E. (2004). Artefacts in the sampling of nitrate studied in the "INTERCOMP" campaigns of EUROTRAC-AEROSOL. *Atmos. Environ.* 38: 6487–6496.

Schmidt, G.A., Kelley, M., Nazarenko, L., Ruedy, R.,

Russell, G.L., Aleinov, I., Bauer, M., Bauer, S.E., Bhat, M.K., Bleck, R., Canuto, V., Chen, Y.H., Cheng, Y., Clune, T.L., Del Genio, A., de Fainchtein, R., Faluvegi, G., Hansen, J.E., Healy, R.J., Kiang, N.Y., Koch, D., Lacis, A.A., LeGrande, A.N., Lerner, J., Lo, K.K., Matthews, E.E., Menon, S., Miller, R.L., Oinas, V., Oloso, A.O., Perlwitz, J.P., Puma, M.J., Putman, W.M., Rind, D., Romanou, A., Sato, M., Shindell, D.T., Sun, S., Syed, R.A., Tausnev, N., Tsigaridis, K., Unger, N., Voulgarakis, A., Yao, M.S. and Zhang, J. (2014). Configuration and assessment of the GISS ModelE2 contributions to the CMIP5 archive. *J. Adv. Model. Earth Syst.* 6: 141–184.

Schmidt, G. A., Ruedy, R., Hansen, J.E., Aleinov, I., Bell, N., Bauer, M., Bauer, S., Cairns, B., Canuto, V., Cheng, Y., Del Genio, A., Faluvegi, G., Friend, A.D., Hall, T.M., Hu, Y., Kelley, M., Kiang, N.Y., Koch, D., Lacis, A. A., Lerner, J., Lo, K.K., Miller, R.L., Nazarenko, L., Oinas, V., Perlwitz, J., Perlwitz, J., Rind, D., Romanou, A., Russell, G.L., Sato, M., Shindell, D.T., Stone, P.H., Sun, S., Tausnev, N., Thresher, D. and Yao, M.S. (2006). Present day atmospheric simulations using GISS ModelE: Comparison to in-situ, satellite and reanalysis data. *J. Clim.* 19: 153–192.

Shen, Z.X., Cao, J.J., Arimoto, R., Zhang, R.J., Jie, D.M., Liu, S.X. and Zhu, C.S. (2007). Chemical composition and source characterization of spring aerosol over Horqin sand land in northeastern China. *J. Geophys. Res.* 112: D14315.

Shindell, D.T., Faluvegi, G., Unger, N. and Aguilar, E. (2006). Simulations of preindustrial, present-day, and 2100 conditions in the NASA GISS composition and climate model G-PUCCINI. *Atmos. Chem. Phys.* 6: 4427–4459.

Shindell, D.T., Lamarque, J.F., Schulz, M., Flanner, M., Jiao, C., Chin, M., Young, P.J., Lee, Y.H., Rotstayn, L. and Mahowald, N. (2013). Radiative forcing in the ACCMIP historical and future climate simulations. *Atmos. Chem. Phys.* 12: 21105–21210.

Sillanpää, M., Hillamo, R., Saarikoski, S., Frey, A., Pennanen, A., Makkonen, U., Spolnik, Z., Grieken, R. V., Braniš, M. and Brunekreef, B. (2006). Chemical composition and mass closure of particulate matter at six urban sites in Europe. *Atmos. Environ.* 40: 212–223.

Sun, Y.L., Zhuang, G.S., Wang, Y., Han, L.H., Guo, J.H., Dan, M., Zhang, W.J., Wang, Z.F. and Hao, Z.P. (2004). The air-borne particulate pollution in Beijing—concentration, composition, distribution and sources. *Atmos. Environ.* 38: 5991–6004.

Tan, J.H., Duan, J.C., Kebin, H.E., Yongliang, M.A., Duan, F.K., Yuan, C. and Jiamo, F.U. (2009). Chemical characteristics of $PM_{2.5}$ during a typical haze episode in Guangzhou. *J. Environ. Sci.* 21: 774–781.

Tang, Y.H., Carmichael, G.R., Seinfeld, J.H., Dabdub, D., Weber, R.J., Huebert, B., Clarke, A.D., Guazzotti, S.A., Sodeman, D.A. and Prather, K.A. (2004). Three-dimensional simulations of inorganic aerosol distributions in east Asia during spring 2001. *J. Geophys. Res.* 109: 1399–1405.

Wang, H.L., Zhou, Y.M., Zhuang, Y.H., Wang, X.K. and Hao, Z.P. (2009). Characterization of $PM_{2.5}$/$PM_{2.5-10}$ and source tracking in the juncture belt between urban and rural areas of Beijing. *Chin. Sci. Bull.* 54: 2506–2515.

Wang, L.L., Wang, S.L., Wang, X.F., Xu, Z., Zhou, S.Z., Yuan, C., Yu, Y.C., Wang, T. and Wang, W.X. (2011). Characteristics of participate matter pollution during August 2009 in Beijing. *China Environ. Sci.* 31: 553–560 (in Chinese).

Wang, T.J., Min, J.Z., Xu, Y.F. and Lam, K.S. (2003). Seasonal variations of anthropogenic sulfate aerosol and direct radiative forcing over China. *Meteorol. Atmos. Phys.* 84: 185–198.

Wang, X.H., Bi, X.H., Sheng, G.Y. and Fu, J.M. (2006a). Chemical Composition and Sources of PM_{10} and $PM_{2.5}$ Aerosols in Guangzhou, China. *Environ. Monit. Assess.* 119: 425–439.

Wang, Y., Zhuang, G.S., Tang, A.H., Yuan, H., Sun, Y.L., Chen, S. and Zheng, A.H. (2005). The ion chemistry and the source of $PM_{2.5}$ aerosol in Beijing. *Atmos. Environ.* 39: 3771–3784.

Wang, Y., Zhuang, G.S., Zhang, X.Y., Huang, K., Xu, C., Tang, A.H., Chen, J.M. and An, Z.S. (2006b). The ion chemistry, seasonal cycle, and sources of $PM_{2.5}$ and TSP aerosol in Shanghai. *Atmos. Environ.* 40: 2935–2952.

Wang, Y., Zhang, Q.Q., He, K., Zhang, Q. and Chai, L. (2013). Sulfate-nitrate-ammonium aerosols over China: Response to 2000–2015 emission changes of sulfur dioxide, nitrogen oxides, and ammonia. *Atmos. Chem. Phys.* 13: 2635–2652.

Xu, J., Bergin, M.H., Yu, X., Liu, G., Zhao, J., Carrico, C. M. and Baumann, K. (2002). Measurement of aerosol chemical, physical and radiative properties in the Yangtze delta region of China. *Atmos. Environ.* 36: 161–173.

Xu, L.L., Chen, X.Q., Chen, J.S., Zhang, F.W., He, C., Zhao, J.P. and Yin, L.Q. (2012). Seasonal variations and chemical compositions of $PM_{2.5}$ aerosol in the urban area of Fuzhou, China. *Atmos. Res.* 104: 264–272.

Yan, P., Zhang, R.J., Ning, H., Zhou, X.J., Zhang, Y.M., Zhou, H.G. and Zhang, L.M. (2012). Characteristics of aerosols and mass closure study at two WMO GAW regional background stations in eastern China. *Atmos. Environ.* 60: 121–131.

Yang, F., Tan, J., Zhao, Q., Du, Z., He, K., Ma, Y., Duan, F., Chen, G. and Zhao, Q. (2011). Characteristics of $PM_{2.5}$ speciation in representative megacities and across China. *Atmos. Chem. Phys.* 11: 5207–5219.

Yang, H., Yu, J.Z., Ho, S.S. H., Xu, J.H., Wu, W.S., Wan, C.H., Wang, X.D., Wang, X.R. and Wang, L.S. (2005). The chemical composition of inorganic and carbonaceous materials in $PM_{2.5}$ in Nanjing, China. *Atmos. Environ.* 39: 3735–3749.

Yang, L.X., Wang, D.C., Cheng, S.H., Wang, Z., Zhou, Y., Zhou, X.H. and Wang, W.X. (2007). Influence of meteorological conditions and particulate matter on visual range impairment in Jinan, China. *Sci. Total Environ.* 383: 164–173.

Yang, L.X., Zhou, X.H., Wang, Z., Zhou, Y., Cheng, S.H., Xu, P.J., Gao, X.M., Nie, W., Wang, X.F. and Wang, W.X. (2012). Airborne fine particulate pollution in Jinan, China: Concentrations, chemical compositions and influence on

visibility impairment. *Atmos. Environ.* 55: 506–514.

Yao, X.H., Chan, C.K., Fang, M., Cadle, S., Chan, T., Mulawa, P., He, K.B. and Ye, B.M. (2002). The water-soluble ionic composition of $PM_{2.5}$ in Shanghai and Beijing, China. *Atmos. Environ.* 36: 4223–4234.

Ye, B.M., Ji, X.L., Yang, H.Z., Yao, X.H., Chan, C.K., Cadle, S.H., Chan, T. and Mulawa, P.A. (2003). Concentration and chemical composition of $PM_{2.5}$ in Shanghai for a 1-year period. *Atmos. Environ.* 37: 499–510.

Ye, X.N. and Chen, J.M. (2009). Advances in the mechanism of secondary fine particulate matters formation. *Prog. Chem.* 21: 288–296.

Zhang, F.W., Xu, L.L., Chen, J.S., Yu, Y.K., Niu, Z.C. and Yin, L.Q. (2012a). Chemical compositions and extinction coefficients of $PM_{2.5}$ in peri-urban of Xiamen, China, during June 2009–May 2010. *Atmos. Res.* 106: 150–158.

Zhang, H.L., Li, J.Y., Ying, Q., Yu, J.Z., Wu, D., Cheng, Y., He, K.B. and Jiang, J.K. (2012b). Source apportionment of $PM_{2.5}$ nitrate and sulfate in China using a source-oriented chemical transport model. *Atmos. Environ.* 62: 228–242.

Zhang, Q., Streets, D.G., Carmichael, G.R., He, K.B., Huo, H., Kannari, A., Klimont, Z., Park, I.S., Reddy, S. and Fu, J.S. (2009a). Asian emissions in 2006 for the NASA INTEX-B mission. *Atmos. Chem. Phys.* 9: 5131–5153.

Zhang, T., Cao, J.J., Tie, X.X., Shen, Z.X., Liu, S.X., Ding, H., Han, Y.M., Wang, G.H., Ho, K.F. and Qiang, J. (2011). Water-soluble ions in atmospheric aerosols measured in Xi'an, China: Seasonal variations and sources. *Atmos. Res.* 102: 110–119.

Zhang, X.Y., Wang, Y.Q., Niu, T., Zhang, X.C., Gong, S.L., Zhang, Y.M. and Sun, J.Y. (2012c). Atmospheric aerosol compositions in China: Spatial/temporal variability, chemical signature, regional haze distribution and comparisons with global aerosols. *Atmos. Chem. Phys.* 12: 779–799.

Zhang, Z.F., Zhu, T., Zhao, D.F., Li, H.J., Zhang, Z.F., Zhu, T. and Li, H.J. (2009b). Heterogeneous reaction of NO_2 on the surface of mineral dust particles. *Prog. Chem.* 21: 282–287.

Zheng, Z.H., Tong, H., Tong, Z.Q., Zhang, J.F. and Huang, Y. (2008). Preparation of low temperature and high activity Mn-V-Ce/TiO_2 catalyst and its catalytic performance on NO oxidation. *Chin. J. Process Eng.* 8: 1205–1212 (in Chinese).

Zhou, Y., Wang, T., Gao, X.M., Xue, L.K., Wang, X.F., Wang, Z., Gao, J., Zhang, Q.Z. and Wang, W.X. (2009). Continuous observations of water-soluble ions in $PM_{2.5}$ at Mount Tai (1534 m asl) in central-eastern China. *J. Atmos. Chem.* 64: 107–127.

Received for review, January 15, 2016
Revised, April 15, 2016
Accepted, April 23, 2016